Multiple Model-Based Control of the Tennessee−Eastman Process

Zhenhua Tian and Karlene A. Hoo*

Department of Chemical Engineering, Texas Tech University, Lubbock, Texas 79409

This work addresses the model-based control of the Tennessee−Eastman (TE) challenge problem using a state-shared model. A detailed mechanistic nonlinear model is developed and validated with data taken from the original Downs and Vogel work [Downs, J. J.; Vogel, E. F. *Comput. Chem. Eng*. **1993**, *17* (3), 245−255] and their accompanying Fortran programs. Two plantwide model predictive control (MPC) strategies that differ in the types of models used are applied to address regulation and transition control. The first employs multiple fixed-parameter models, identified at known grades, and the second uses an adaptive state-shared model [Tian, Z.; Hoo, K. A. *Comput. Chem. Eng*. **2003**, *27* (11), 1641−1656] constructed from three fixed-parameter models and one specialized adaptive model. The first MPC strategy demonstrates closed-loop regulation and grade-transition performance especially when the worst disturbance, the loss of the A feed, is present. The second MPC strategy provides a better closed-loop performance for grade transitions when compared with the first MPC strategy.

1. Introduction

The Tennessee−Eastman (TE) challenge problem provides a plant flowsheet (see Figure 1), seven possible operating states of three product grades, a list of expected disturbances, and a Fortran-based computer program that represents implicit dynamic models of the unit operations present in the flowsheet.[1]

The multiple operating states pose a significant transition control problem, while the different types of disturbances present a challenging regulation problem. Since the initial publication of the TE process more than 10 years ago,[1] at least 60 publications have appeared in the open literature in which a plethora of control formulations have been tried, as well as statistical process monitoring, sensor fault detection, and optimal scheduling.[3−9]

McAvoy and Ye[10] developed a decentralized plantwide control design based on multiple single input/single output (SISO) control loops. The methodology involved the screening of various pairs of control and manipulated variables using steady-state techniques, such as relative gain array.[11] Ricker and Lee[7] tested this strategy and found that the compressor power loop is often saturated during transient operations. This control scheme did not demonstrate transition control among the three product grades and among the different operating modes.

Luyben and co-workers[5] used their nine-step plantwide control design approach to develop SISO feedback control loops for both on-demand production and on-supply of reactants. The control system developed is demonstrated for regulation. In the case of the extreme disturbances (e.g., loss of the A feed), the usual industrial mode of applying overrides and high and low selectors is applied. This control scheme also did not address grade-transition control. Papers related to this work can be found in refs 12 and 13.

The most extensive studies of the TE process have been reported by Ricker and co-workers. Ricker and Lee[8] have derived nonlinear, mechanistic models of the major unit operations that reproduced the essential dynamic process characteristics. However, a key simplification, omission of the energy balance, is applied. An extended Kalman filter is developed to provide continuous adjustments of the dynamic model parameters (and states) during transients. This simplified model was used by Ricker and Lee[7] to formulate an MPC controller. The control strategy when compared with the typical SISO multiloop strategy shows a better closed-loop performance especially for transition control (grade and operating state changes) and constraint handling. Although the models that represent the plant are nonlinear, MPC uses approximate linear models found by linearization of the nonlinear models at every sample point. In this fashion, MPC uses linear time-varying models of the plant.

In ref 9, Ricker developed a decentralized control structure that gave results superior to those in the study done in ref 7. Ricker suggests that the most important criterion for a successful control strategy lies with the selection of the set of controlled variables. Similar statements in this regard can be found in the publications of Skogestad and co-workers[13−15] and Shinnar and co-workers.[16−18]

Besides the base mode, there are six optimal steady-state modes of process operation for three different production mass ratios (see Table 1). This work addresses disturbance rejection at known operating modes and transition control among the three product grades.

The organization of the rest of the paper is as follows. Section 2 presents a very brief overview of the TE process necessary to understand the process and the control development. More details can be found in the Appendix. Section 3 provides the detailed mechanistic nonlinear model development. Section 4 presents a system analysis of the models in section 3. Section 5 presents two approaches to MPC. The first uses fixed-parameter linear models identified at the known operating modes and switching to demonstrate the performance of the controller for regulation and single and multiple transitions among the product grades. The second uses an adaptive state-shared linear model

* To whom correspondence should be addressed. E-mail: khoo@coe.ttu.edu.

10.1021/ie0496939 CCC: $30.25
Published on Web 03/11/2005

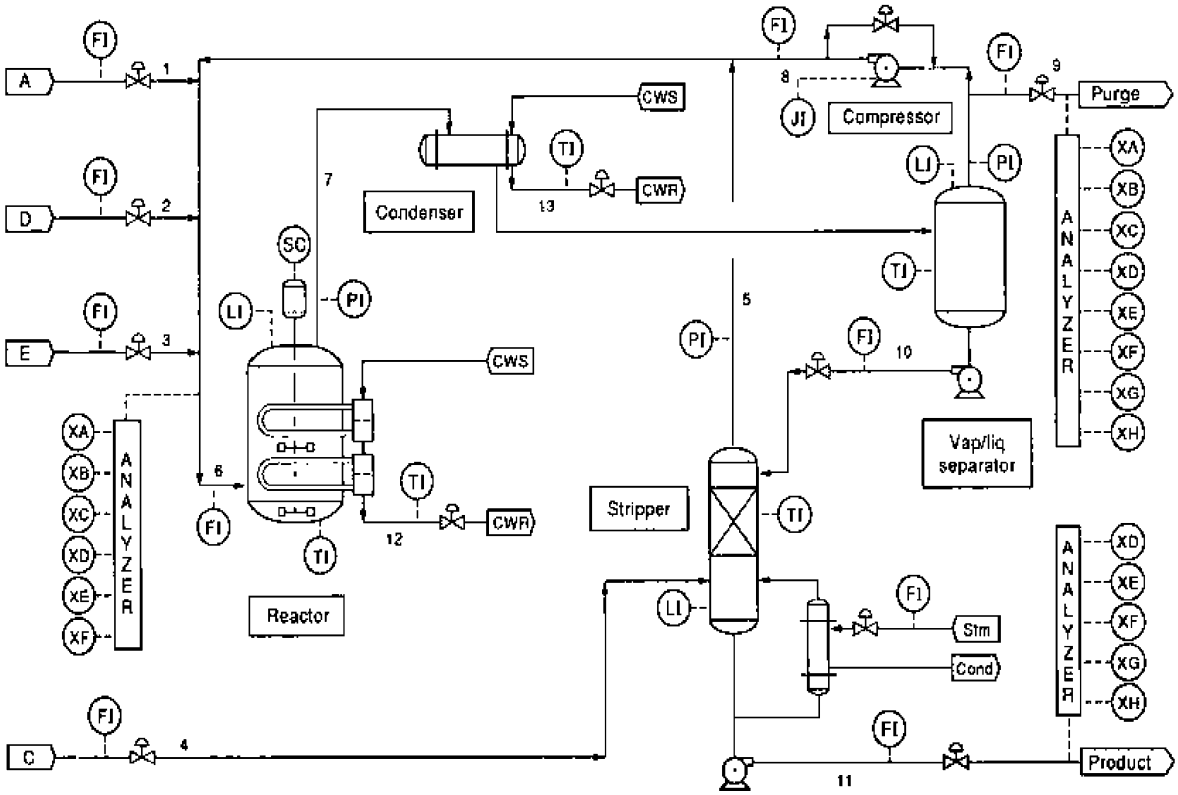

Figure 1. TE process design flowsheet.[1] There are 5 major unit operations (the chemical reactor, condenser, separator, stripper, and compressor), 41 measurements, and 12 control degrees of freedom.

Table 1. Seven Modes of Process Operation

mode	G/H mass ratio	production rate (stream 11), kg h^{-1}
0, 1	50/50	7038 G/7038 H
2	10/90	1048 G/12669 H
3	90/10	10000 G/1111 H
4	50/50	maximum production rate
5	10/90	maximum production rate
6	90/10	maximum production rate

approach. Last, a summary of the work and concluding remarks are provided in section 6.

2. Process Description

A process description is provided by Downs and Vogel.[1] The TE process has five major unit operations: a chemical reactor, a product condenser, a vapor−liquid separator, a product stripper, and a recycle compressor (see Figure 1).

The process produces two products from four exothermic, irreversible reactions. There are a total of eight components labeled as A−H, with component B an inert, components G and H the primary products, and component F a byproduct. The chemical reactions provided are

$$\begin{aligned} 1.\ & A(g) + C(g) + D(g) \rightarrow G(l) \\ 2.\ & A(g) + C(g) + E(g) \rightarrow H(l) \\ 3.\ & A(g) + E(g) \rightarrow F(l) \\ 4.\ & 3D(g) \rightarrow 2F(l) \end{aligned} \quad (1)$$

The reaction rates are a function of the temperature through an Arrhenius expression. Reaction 1 has a higher activation energy (2 times larger) when compared to reaction 2 and thus a greater sensitivity to temperature changes. The reactions are approximately first-order with respect to each reactant concentration.

The reactor is modeled as an ideal continuous stirred tank reactor (CSTR) with internal cooling to remove the heat of reaction. A nonvolatile catalyst is dissolved in the liquid phase. The products have moderate volatility and exit the reactor with the unreacted gases. The catalyst remains in the reactor. The reactor product stream, a vapor, is first passed through a water-supplied condenser before entering the vapor−liquid separator. The noncondensable components are returned to the reactor by way of a centrifugal compressor. The condensed components are sent to the stripping column to remove the remaining reactants. The product components, G and H, exit at the stripper base (stream 11 in Figure 1). The inert component, B, and the byproduct component, F, primarily exit the system as vapors from the vapor−liquid separator.

Table 1 lists the seven modes of process operation at three different G/H mass ratios.

Mode 0 is the *base case*. Modes 1−3 are operating states at the minimum operating costs at the three different G/H mass ratios. Modes 4−6 are operating states at the maximum production rate of the three different G/H mass ratios. The product mix is dictated by demand. The plant production rate is set by market demand or capacity limitation. A detailed description of the process is provided in the Appendix.

The steady-state energy balances of each unit operation are provided in the computer program supplied with the process flowsheet description. This work assumes that this computer program is correct; thus, the results found at the different operating modes form the basis from which to validate any other representation of the flowsheet. Starting from a mechanistic point of view, mechanistic models of the unit operations are

developed based on explicit material and energy balances. Subsequently, these mechanistic models are solved numerically, and their results are validated against the results of the original Downs and Vogel Fortran programs. The proposed model reveals the mechanisms and principles in a straightforward manner that may enable other advanced and different studies that may not have been easy with the Fortran code of Downs and Vogel. In this work, the mechanistic model is used as the surrogate for the nonlinear plant.

3. Mechanistic Model Development

3.1. Model Assumptions. The assumptions provided by the TE problem are as follows:

(i) The vapor-phase species are assumed to behave as ideal gases.

(ii) The vapor−liquid equilibrium follows Raoult's law[19]

$$P_i = Py_i = P_{\mathrm{vp},i}x_i^{\sigma} \tag{2}$$

where P is the total pressure, $P_{\mathrm{vp},i}$ is the saturated vapor pressure of component i, and y_i and x_i^{σ} are the mole fractions of component i in the vapor and liquid phases, respectively.

The vapor pressure is calculated by Antoine's equation[19]

$$P_{\mathrm{vp}} = \exp\left(A + \frac{B}{T + C}\right) \tag{3}$$

where P_{vp} and T have units of mmHg and °C, respectively. The coefficients of Antoine's equation for the components of this system are listed in Table 10 (the values provided in this table are taken from Downs and Vogel's Fortran programs).

(iii) All phases are well mixed.

(iv) The rates of reaction are proportional to the partial pressures of the reactant in each reaction.

(v) All reactions occur in the vapor phase, and the rates of reaction are proportional to the vapor volume in the reactor. Components A−C are insoluble in all liquid phases (noncondensable).

(vi) Where liquid and vapor phases coexist, vapor−liquid equilibrium is assumed.

(vii) The phase of the feed mixing zone (stream 6 in Figure 1; the feed mixing zone consists of five streams that together become the feed to the reactor) is entirely vapor. The condition of well-mixedness is assumed in the mixing zone.

(viii) The reactor agitator only affects the degree of heat transferred reflected in the value of the heat-transfer coefficient.

3.2. State-Space Formulation. A nonlinear state-space model with the form

$$\dot{\mathbf{x}}_{\mathrm{p}}(t) = \mathbf{f}[\mathbf{x}_{\mathrm{p}}(t),\mathbf{u}_{\mathrm{p}}(t),t] \tag{4}$$

$$\mathbf{y}_{\mathrm{p}}(t) = \mathbf{g}[\mathbf{x}_{\mathrm{p}}(t),\mathbf{u}_{\mathrm{p}}(t),t] \tag{5}$$

is developed where $t \in R^+$, $\mathbf{x}_{\mathrm{p}}(t) \in X$ are the states with $X \subset R^n$, a *compact* set, $\mathbf{y}_{\mathrm{p}}(t) \in Y$ are the measured outputs with $Y \subset R^p$, and $\mathbf{u}_{\mathrm{p}}(t) \in U$ are the manipulated variables with $U \subset R^m$, a *compact* and *convex* set.[20] The vector functions $\mathbf{f}$ and $\mathbf{g}$ are defined by $\mathbf{f}$: $R^n \times R^m \times R^+ \rightarrow R^n$ and $\mathbf{g}$: $R^n \times R^m \times R^+ \rightarrow R^p$.

Let the vector $\mathbf{x}_{\mathrm{p}}{}^{\mathrm{T}}$ represent the states arranged as follows:

$$\mathbf{x}_{\mathrm{p}}{}^{\mathrm{T}} = [N_{\mathrm{A,r}}, N_{\mathrm{B,r}}, ..., N_{\mathrm{H,r}}, T_{\mathrm{r}}, N_{\mathrm{A,s}}, N_{\mathrm{B,s}}, ..., N_{\mathrm{H,s}}, T_{\mathrm{s}}, N_{\mathrm{A,c}}, N_{\mathrm{B,c}}, ..., N_{\mathrm{H,c}}, T_{\mathrm{c}}, N_{\mathrm{A,v}}, N_{\mathrm{B,v}}, ..., N_{\mathrm{H,v}}, T_{\mathrm{v}}, T_{\mathrm{cwr}}, T_{\mathrm{cws}}]$$

where $N_{i,\mathrm{r}}$ is the molar holdup (lb·mol) of component i = A, ..., H in the reactor and $N_{i,\mathrm{s}}$, $N_{i,\mathrm{c}}$, and $N_{i,\mathrm{v}}$ are the molar holdups in the separator, stripper, and feed mixing zone, respectively. The temperatures (°C) in the reactor, separator, stripper, and mixing zone are T_{r}, T_{s}, T_{c}, and T_{v}, respectively. The reactor and condenser cooling water outlet temperatures (°C) are T_{cwr} and T_{cws}, respectively. There are 38 states and 12 *control degrees of freedom* (11 control valves and the agitator speed).

For presentation purposes, the TE process is compartmentalized into four subsystems, namely, a reaction subsystem, a separation subsystem, a stripping subsystem, and a fictitious mixing zone. Also, the conservation equations are established based on each unit operation in a subsystem and, hence, the boundaries of the subsystems are not necessarily the boundaries of the conservation equations.

3.3. Reaction System. The reactor is a CSTR that holds two phases, liquid and vapor, which are assumed to be at equilibrium. Heat generated by the four exothermic chemical reactions (see eq 1) is removed by a heat exchanger internal to the reactor. Both the feed and the product streams of the reactor are vapor streams.

Eight component balances can be written for the reactor in the form given by

$$\frac{\mathrm{d}N_{i,\mathrm{r}}}{\mathrm{d}t} = y_{i,6}F_6 - y_{i,7}F_7 + \sum_{j=1}^{4} v_{ij}R_j, \quad i = \mathrm{A}, ..., \mathrm{H} \tag{6}$$

where F_k is the molar flow rate of stream k, $y_{i,k}$ is the mole fraction of component i in stream k, v_{ij} is the stoichiometric coefficient of component i in reaction j, and R_j is the reaction rate of reaction j in the reactor (lb·mol/h). Note that the subscripts match those found in Figure 1.

The four chemical reaction rates are given as

$$R_1 = \exp(\beta_1)V_{\mathrm{V,r}}P_{\mathrm{A,r}}{}^{\alpha_1}P_{\mathrm{C,r}}{}^{\alpha_2}P_{\mathrm{D,r}}\exp(-E_1/RT_{\mathrm{r}})$$

$$R_2 = \exp(\beta_2)V_{\mathrm{V,r}}P_{\mathrm{A,r}}{}^{\alpha_1}P_{\mathrm{C,r}}{}^{\alpha_2}P_{\mathrm{E,r}}\exp(-E_2/RT_{\mathrm{r}})$$

$$R_3 = \exp(\beta_3)V_{\mathrm{V,r}}P_{\mathrm{A,r}}P_{\mathrm{E,r}}\exp(-E_3/RT_{\mathrm{r}})$$

$$R_4 = \exp(\beta_4)V_{\mathrm{V,r}}P_{\mathrm{A,r}}P_{\mathrm{D,r}}\exp(-E_4/RT_{\mathrm{r}}) \tag{7}$$

where $P_{i,\mathrm{r}}$, i = A, ..., H, is the partial pressure of component i in the vapor phase, $V_{\mathrm{V,r}}$ is the vapor volume in the reactor, and $\exp(\beta_i)$, i = 1, ..., 4, is the frequency factor. Note that $\exp(\beta_i)$ is not dimensionless. Values of these parameters are given in Table 12 (the values provided in this table are taken from Downs and Vogel's Fortran program).

The energy balance for the reactor is given by

$$\frac{\mathrm{d}H_{\mathrm{r}}}{\mathrm{d}t} = h_6F_6 - h_7F_7 + R_1(-Q_{\mathrm{r1}}) + R_2(-Q_{\mathrm{r2}}) + Q_{\mathrm{ur}} \tag{8}$$

where h_k is the specific molar enthalpy of stream k = 6

and 7, Q_{r1} and Q_{r2} are the molar heats of reaction for reactions 1 and 2, respectively, and Q_{ur} is the heat-transfer rate. The reactor enthalpy H_r can also be found from

$$H_r(T_r) = h_r(T_r)\sum_{i=D}^{H} N_{i,r} \tag{9}$$

where h_r is the specific molar enthalpy of the liquid mixture.

Because the material holdup in the vapor phase of the reactor is much smaller than that in the liquid phase, the energy in the vapor phase is assumed negligible. The reaction rates of the product reactions (1 and 2) are larger than those of the byproduct reactions (3 and 4). Thus, the heat generated by the byproduct reactions is assumed negligible.

Heat transfer between the internal heat exchanger and the reactor is given by

$$Q_{ur} = UA(T_r - T_{out}) \tag{10}$$

The heat-transfer coefficient U is affected by the agitation rate, and A is the contact area.

The empirical relationship (from the original Downs and Vogel's Fortran programs) for the dimensionless agitator speed, v_{ag}, is given by

$$v_{ag} = \chi_{ag}\mathrm{Cap} + 1.5 \tag{11}$$

where χ_{ag} is the fraction of the maximum agitator capacity.

The empirical relationship (from the original Downs and Vogel's Fortran programs) for the product of the heat-transfer coefficient and the heat-transfer area is given by

$$UA = \begin{cases} 1 & L_r > 60\%\, L_{r,tot} \\ 0 & L_r < 10\%\, L_{r,tot} \\ 0.85549(0.025V_{L,r}/7.8 - 0.25) & \\ \quad \times (-0.5v_{ag}^{\,2} + 2.75v_{ag} - 2.5) & \text{otherwise} \end{cases} \tag{12}$$

where L_r is the liquid level and $L_{r,tot}$ is the maximum feasible liquid level of the reactor.

The following empirical equations (from the original Downs and Vogel's Fortran programs) are used to calculate the specific molar enthalpy of the mixture

$$h_{liq}(T) = \sum_{i=A}^{H} x_i \mathrm{MW}_i(\mathrm{AH}_i T + \mathrm{BH}_i T^2/2 + \mathrm{CH}_i T^3/3)$$

$$h_{vap}(T) = \sum_{i=A}^{H} y_i \mathrm{MW}_i(\mathrm{AG}_i T + \mathrm{BG}_i T^2/2 + \mathrm{CG}_i T^3/3 + \mathrm{AV}_i) \tag{13}$$

where x_i and y_i are the mole fractions of component i in the liquid and vapor phases, respectively, and MW_i is the molecular weight of component i. The coefficients of the above equations are provided in Downs and Vogel's Fortran programs.

Substitution of eq 13 into eq 9 gives

$$H_r = \sum_{i=D}^{H} N_{i,r} \sum_{i=A}^{H} x_{i,r} \mathrm{MW}_i(\mathrm{AH}_i T_r + \mathrm{BH}_i T_r^{\,2}/2 + \mathrm{CH}_i T_r^{\,3}/3)$$

Taking the total derivative of the above equation in accordance with the left-hand side of eq 8 gives

$$\frac{dH_r}{dt} = \sum_{i=D}^{H} \frac{dN_{i,r}}{dt} \sum_{i=A}^{H} x_{i,r} \mathrm{MW}_i(\mathrm{AH}_i T_r + \mathrm{BH}_i T_r^{\,2}/2 + \mathrm{CH}_i T_r^{\,3}/3) + \sum_{i=D}^{H} N_{i,r} \sum_{i=A}^{H} x_{i,r} \mathrm{MW}_i(\mathrm{AH}_i + \mathrm{BH}_i T_r + \mathrm{CH}_i T_r^{\,2}) \frac{dT_r}{dt} + \sum_{i=D}^{H} N_{i,r} \sum_{i=A}^{H} \mathrm{MW}_i(\mathrm{AH}_i T_r + \mathrm{BH}_i T_r^{\,2}/2 + \mathrm{CH}_i T_r^{\,3}/3) \frac{dx_{i,r}}{dt} \tag{14}$$

For the condensable species, $x_{i,r} = N_{i,r}/\sum_{j=D}^{H} N_{j,r}$, i = D, ..., H. Thus

$$\frac{dx_{i,r}}{dt} = \frac{d}{dt}\left(\frac{N_{i,r}}{\sum_{j=D}^{H} N_{j,r}}\right) = \frac{\frac{dN_{i,r}}{dt}\sum_{j=D}^{H} N_{j,r} - N_{i,r}\left(\sum_{j=D}^{H} \frac{dN_{j,r}}{dt}\right)}{(\sum_{j=D}^{H} N_{j,r})^2} \tag{15}$$

Let

$$\hat{C}_{pr} \equiv \sum_{i=A}^{H} x_{i,r} \mathrm{MW}_i(\mathrm{AH}_i + \mathrm{BH}_i T_r + \mathrm{CH}_i T_r^{\,2})$$

represent the specific molar heat capacity of the liquid mixture in the reactor. Substituting eqs 14 and 15 into eq 8 gives

$$\frac{dT_r}{dt} = \left(h_6 F_6 - h_7 F_7 + R_1(-Q_{r1}) + R_2(-Q_{r2}) + Q_{ur} - \sum_{i=D}^{H} \frac{dN_{i,r}}{dt} h_r - \sum_{i=D}^{H} N_{i,r} \sum_{i=D}^{H} \frac{h_{i,r}}{x_{i,r}} \frac{dx_r(i)}{dt}\right) / \hat{C}_{pr} \sum_{i=D}^{H} N_{i,r} \tag{16}$$

where $h_{i,r}$, the specific molar enthalpy of component i in the liquid mixture in the reactor, is determined from the following expression:

$$h_{i,r} = x_{i,r} \mathrm{MW}_i(\mathrm{AH}_i T_r + \mathrm{BH}_i T_r^{\,2}/2 + \mathrm{CH}_i T_r^{\,3}/3)$$

Note that for components D−H the term $N_{i,r}$ refers to the number of moles in the liquid phase. Accumulation of these components in the vapor phase is assumed negligible.

The liquid volume, $V_{L,r}$, of the reactor can be obtained from

$$V_{L,r} = \frac{\sum_{i=D}^{H} N_{i,r}}{\rho_{liq,r}(T_r)} \tag{17}$$

where $\rho_{liq,r}$ is the density of the liquid in the reactor. By difference, the vapor volume, $V_{V,r}$, is the difference between the reactor volume and the liquid volume

$$V_{V,r} = V_r - V_{L,r} \tag{18}$$

The densities of the liquid in the reactor, the separator, and the stripper are determined from the following empirical equation:

$$\rho_{liq}(T) = \left(\sum_{i=A}^{H} \frac{x_i MW_i}{AD_i + BD_i T + CD_i T^2} \right)^{-1} \tag{19}$$

where the above equation and its coefficients are taken from the original Downs and Vogel's Fortran programs.

Equations 2 and 3 are used to calculate the vapor and partial pressures of components D−H. The *ideal gas law* is used to calculate the partial pressures of the noncondensables

$$P_{i,r} = \frac{N_{i,r} R T_r}{V_{V,r}}, \quad i = A-C \tag{20}$$

The total pressure in the vapor phase is found from the summation of the partial pressures

$$P_r = \sum_{i=A}^{H} P_{i,r} \tag{21}$$

The mole fraction of component i in the vapor phase can be calculated from a ratio of the partial and total pressures

$$y_{i,r} = P_{i,r}/P_r, \quad i = A, ..., H \tag{22}$$

The reactor input and output streams, F_6 and F_7 (see Figure 1), are proportional to the square root of the pressure difference at the inlet and outlet of the reactor

$$F_6 = 1937.6 \frac{\sqrt{P_v - P_r}}{MWS_6} \qquad F_7 = 4574.21 \frac{\sqrt{P_v - P_r}}{MWS_7}$$

where P_v and P_s are the pressures in the mixing zone and separator, respectively, and the coefficients of the above equations are taken from the original Downs and Vogel's Fortran programs. The term MWS_i is the molecular weight of stream i determined from

$$MWS_i = \sum_{j=A}^{H} x_{j,i} MW_j, \quad i = 1, ..., 11 \tag{23}$$

where $x_{j,i}$ is the mole fraction of component j in stream i.

The energy balance on the reactor internal cooling system is given by

$$C_{pc} \rho_c V_{cool} \frac{dT_{out}}{dt} = C_{pc} \rho_c (T_{in} - T_{out}) F_{wr} - Q_{ur} \tag{24}$$

where ρ_c is the molar density of the cooling water, V_{cool} is the cooling water system volume, and F_{wr} is the cooling water flow rate, which is a function of the valve position.

Equations 6, 16, and 24 represent the nonlinear dynamic model of the reactor system.

3.4. Separation System. The separation system includes the vapor−liquid separator, the product condenser, and the recycle compressor. A mathematical model that describes the behavior of the vapor−liquid separator is similar to the reactor model, but without the chemical reactions.

The component balances for the separator are given by

$$\frac{dN_{i,s}}{dt} = y_{i,7} F_7 - y_{i,8} F_8 - y_{i,9} F_9 - x_{i,10} F_{10}, \quad i = A, ..., H \tag{25}$$

where the notation is as before. The energy balance for the separator is given by

$$\frac{dT_s}{dt} = \left(h_7 F_7 - h_8 F_8 - h_9 F_9 - h_{10} F_{10} + W_c + Q_{us} - \sum_{i=D}^{H} \frac{dN_{i,s}}{dt} h_s - \sum_{i=D}^{H} N_{i,s} \sum_{i=D}^{H} \frac{h_{i,s}}{x_{i,s}} \frac{dx_{i,s}}{dt} \right) / \hat{C}_{ps} \sum_{i=D}^{H} N_{i,s} \tag{26}$$

where $Q_{us} = UA_s(T_{out,s} - T_{st,7})$. W_c is the power of the compressor, Q_{us} is the energy transferred between the condenser cooling water system and stream 7, $T_{st,7}$ is the temperature of stream 7, and $T_{out,s}$ is the exit temperature of the water leaving the condenser. The product of the heat-transfer coefficient and the heat-transfer area is given by (from the original Downs and Vogel's Fortran programs)

$$UA_s = 0.404655 \left[1.0 - \frac{1.0}{1.0 + (F_7/3528.73)^4} \right] \tag{27}$$

The flow rates of the exit streams are functions of the pressure differences

$$F_8 = \left\{ \left(1 - \frac{1}{1.197} \right) \left[1.0 - \left(\frac{P_v}{P_s} \right)^3 \right] - 53.349 \chi_5 \sqrt{P_s - P_o} \right\} / MWS_8$$

$$F_9 = 0.151169 \chi_6 \sqrt{P_s - P_o} / MWS_9$$

$$F_{10} = 1500 \chi_7 / 100 \tag{28}$$

where P_o is standard atmospheric pressure and χ_j, j = 5−7, is the valve coefficient of stream j as supplied by the manufacturer.

The empirical equation (from the original Downs and Vogel's Fortran programs) used to calculate the work done by the compressor (compressor characteristic curve) is given as

$$W_c = \frac{\left(1 - \frac{1}{1.197} \right) \left[1.0 - \left(\frac{P_v}{P_s} \right)^3 \right] T_s (P_v - P_s)}{MWS_8 P_s} \tag{29}$$

The energy balance in the condenser is given by

$$C_{pc} \rho_s V_{cool} \frac{dT_{out,s}}{dt} = C_{pc} \rho_s (T_{in,s} - T_{out,s}) F_{ws} - Q_{us} \tag{30}$$

where ρ_s is molar density of the cooling water, V_{cool} is

the condenser volume, and F_{ws} is the cooling water flow rate, which is a function of its valve position.

Antoine's equation, the ideal gas law, and Raoult's law are used to determine the amount of each component in the liquid and vapor phases, their partial pressures, and the liquid levels. Equations 25−30 represent the nonlinear dynamic model of the separator system.

3.5. Stripping System. The information provided about the stripper operation is minimal. The component balances for the splitter are given by

$$\frac{dN_{i,c}}{dt} = y_{i,4}F_4 + x_{i,10}F_{10} - y_{i,5}F_5 - x_{i,11}F_{11}, \quad i = A, ..., H \quad (31)$$

and

$$F_5 = \sum_{i=A}^{H} \Phi_i (y_{i,4}F_4 + x_{i,10}F_{10}) \quad (32)$$

where $\Phi_j, j = A, ..., H$, are the component splits for the exiting vapor stream (stream 5). Nominal values of the component splits are given in Table 11.

The following empirical equations (from the original Downs and Vogel's Fortran programs)

$$\Phi_D = \frac{8.5010(F_4/F_{10})f_{T_c}}{1 + 8.5010(F_4/F_{10})f_{T_c}}$$

$$\Phi_E = \frac{11.402(F_4/F_{10})f_{T_c}}{1 + 11.402(F_4/F_{10})f_{T_c}}$$

$$\Phi_F = \frac{11.795(F_4/F_{10})f_{T_c}}{1 + 11.795(F_4/F_{10})f_{T_c}}$$

$$\Phi_G = \frac{0.0480(F_4/F_{10})f_{T_c}}{1 + 0.0480(F_4/F_{10})f_{T_c}}$$

$$\Phi_H = \frac{0.0242(F_4/F_{10})f_{T_c}}{1 + 0.0242(F_4/F_{10})f_{T_c}} \quad (33)$$

where

$$f_{T_c} = \begin{cases} T_c - 120.262 & T_c \geq 170\ ^\circ C \\ 0.1 & T_c \leq 5.292\ ^\circ C \\ \dfrac{363.744}{177 - T_c} - 2.22579488 & \text{otherwise} \end{cases}$$

are used to determine the splits for components D−H as a function of the stripper temperature and the flow rates of streams 4 and 10 if the flow rate of stream 10 is larger than 0.1 lb·mol/h.

The energy balance is given by

$$\frac{dT_c}{dt} = \left(h_4F_4 + h_{10}F_{10} - h_5F_5 - h_{11}F_{11} + Q_{uc} - \sum_{i=D}^{H} \frac{dN_{i,c}}{dt} h_c - \sum_{i=D}^{H} N_{i,c} \sum_{i=D}^{H} \frac{h_{i,c}}{x_{i,c}} \frac{dx_{i,c}}{dt} \right) \Big/ \hat{C}_{pc} \sum_{i=D}^{H} N_{i,c} \quad (34)$$

where Q_{uc} is the energy supplied by the stream

$$Q_{uc} = UA_c(100 - T_c) \qquad T_c > 100\ ^\circ C$$

If the temperature in the stripper is greater than 100 °C, there will be no heat transfer. Equations 31 and 34 represent the nonlinear dynamic model of the stripper.

3.6. Mixing Zone. There is no physical mixer unit operation in the TE flowsheet. The fictitious mixing zone represents the point at which five gas streams (1−3, 5, and 8) are mixed prior to becoming the feed to the reactor (stream F_6). The condition of well-mixedness is assumed in the mixing zone.

The component and energy balances are given by

$$\frac{dN_{i,v}}{dt} = y_{i,1}F_1 + y_{i,2}F_2 + y_{i,3}F_3 + y_{i,5}F_5 + y_{i,8}F_8 - y_{i,6}F_6, \quad i = A, ..., H \quad (35)$$

$$\frac{dT_v}{dt} = (\hat{C}_{pv} \sum_{i=A}^{H} N_{i,v})^{-1} \left(h_1F_1 + h_2F_2 + h_3F_3 + h_5F_5 + h_8F_8 - h_6F_6 - \sum_{i=A}^{H} \frac{dN_{i,v}}{dt} h_v - \sum_{i=A}^{H} N_{i,v} \sum_{i=A}^{H} \frac{h_{i,v}}{x_{i,v}} \frac{dy_{i,v}}{dt} \right) \quad (36)$$

Tables 5 and 6 provide definitions of the notation used in the equations.

4. System Analysis

MPC is an advanced controller design that has been implemented successfully in the petrochemical industries over the past 20 years. As such, the details of the linear formulation of MPC will not be repeated here. The interested reader is referred to the work in ref 21 for more information.

In this work, the MPC formulation is based on multiple linear, fixed-parameter, state-space models or an adaptive state-shared linear model of the TE process. The mathematical models developed in section 3 represent a system of nonlinear differential and algebraic equations. To obtain linear models, a numerical linearization [MATLAB/SIMULINK (Mathworks, Natick, MA) routine LINMOD] is used. The linearized model obtained has the following form:

$$\dot{\mathbf{x}} = \mathbf{Ax} + \mathbf{Bu}$$

$$\mathbf{y} = \mathbf{Cx} + \mathbf{Du}$$

$$\mathbf{x} = \mathbf{x}_p - \bar{\mathbf{x}} \qquad \mathbf{y} = \mathbf{y}_p - \bar{\mathbf{y}}_p \qquad \mathbf{u} = \mathbf{u}_p - \bar{\mathbf{u}} \quad (37)$$

where $\bar{\mathbf{x}}$, $\bar{\mathbf{y}}_p$, and $\bar{\mathbf{u}}$ are the steady-state values of $\mathbf{x}_p$, $\mathbf{y}_p$, and $\mathbf{u}_p$, respectively, $\mathbf{A}$ is the Jacobian with respect to the states, $\mathbf{B}$ is the Jacobian with respect to the manipulated variables, and $\mathbf{C}$ and $\mathbf{D}$ are found from a

Table 2. Tuning Parameters for SISO Level Loops and Reactor Temperature

controlled variable	manipulated variable	controller gain	integral time, min
reactor temp (°C)	reactor cooling valve	−0.5%/°C	60
reactor level (%)	D feed flow valve	4%/%	60
separator level (%)	separator effluent valve	−5%/%	60
stripper level (%)	stripper effluent valve	−1.5%/%	60

linearization of the measurement equation (eq 5) with respect to the states and manipulated variables.

An eigenvalue analysis of the dynamic matrix **A** that results from the linearization at the base case values reveals four positive eigenvalues. These eigenvalues can be attributed to the levels of the reactor, separator, and stripper and the reactor temperature.[7,9] Four SISO proportional−integral (PI) feedback controllers are used to regulate the four variables and are configured as follows:

(i) Reactor liquid level: D feed (stream 2) valve.

(ii) Separator liquid level: separator effluent (stream 10) valve.

(iii) Stripper bottoms liquid level: stripper effluent (stream 11) valve.

(iv) Reactor temperature: reactor cooling water valve (stream 12).

The choice of the cooling water valve to control the reactor temperature is based on the proximity rule.[5] That is, the cooling water valve's location provides a rapid response to thermal disturbances.

Within the MPC control strategy, the set point of the reactor temperature becomes a controlled variable; thus, the reactor temperature set point is provided by the MPC. The role of the PI controller is to manipulate the valve position (ultimately the flow rate) to compensate for errors between the reactor temperature and its set point. Tuning parameters (see ref 22, Chapter 13, pp 298−309) for these four SISO loops are listed in Table 2.

Because there are four feedback loops but only the set point of the reactor temperature loop will be under the supervision of the MPC strategy, a linear model for the MPC strategy that reflects these modifications will be obtained by linearizing the 36-state nonlinear model. From the work of Ricker and Lee,[7] it was found that obtaining a linear model with three embedded PI loops will result in large steady-state offsets.

At the three-operating-points base case, 50/50 (modes 0 and 1), 10/90 (mode 2), and 90/10 (mode 3) in Table 1, the eigenvalues of the three resulting linear dynamic matrices are all negative; hence, the linear system is open-loop stable, and the nonlinear system is locally stable.

It is observed that the reactor pressure responds instantaneously to changes in the reactor temperature because temperature variations affect the vapor pressures of each component. Thus, there is one nonzero element in the **D** matrix in the measurement equation (eq 5). The nonzero elements in the **D** matrix represent those inputs that directly affect the outputs, bypassing the dynamic matrix. The MPC formulation requires that this matrix **D** contain only zeroes, i.e., no pass-through inputs. Following the approach proposed in ref 7, an independent, linear, first-order filter with unity filter gain and a time constant of $^1/_{300}$ h is introduced to filter the pressure measurement. When the filter is combined with the above linear model, the number of states is increased by 1. Similarly, because stream 11 directly affects the production rate, a first-order filter with unity filter gain and a time constant of $^1/_{300}$ h also is introduced. Thus, the number of states also is increased by 1.

Table 3. Output Weighting

variable	output weight
reactor pressure	0.1
separator temperature	1.0
separator pressure	0.1
production rate	2.0
stripper temperature	0.5
% A in the purge	0.5
% G in the product	0.1

5. Model-Based Control Framework

In section 3.2, it was pointed out that the plant has 12 control degrees of freedom. These correspond to variables XMV(1)−XMV(12) in Table 7. Table 13 lists 41 measurements. Of the 41, 19 are analyzer measurements that are neither timely nor dependable. This work will assume that, in the purge stream (stream 9), only component A is selected as a controlled variable and, in the product stream (stream 11), only component G is selected as a controlled variable. This eliminates 17 of the 41 measurements from consideration as controlled variables.

The analysis in section 4 shows that the levels of the reactor, separator, and stripper unit operations must be regulated by valves XMV(1), XMV(7), and XMV(8), respectively (see Table 2). Additionally, the reactor temperature must be regulated; the reactor cooling water valve, XMV(10), is assigned this task. Because the agitator speed, XMV(12), only affects the energy transfer of the reactor system, it is intuitive that the agitator speed be set to its maximum value. That is, the higher the speed, the greater the heat transferred. This also was confirmed by the studies in refs 7 and 13. In the study in ref 5, a different strategy was proposed for the agitator speed.

For product purity control (regulate the G/H ratio), the G component in the product stream will be selected as a controlled variable. From the known reactions, the product ratio can be regulated by a ratio of the E to D feed [XMV(2) and XMV(1)] rates (only 1 degree of freedom is assigned for G/H ratio control). For operating cost control, the A component in the purge stream will be regulated. At this point, 7 control degrees of freedom are assigned; thus, only 5 of the remaining 12 measured variables can be selected as controlled variables. From among these, the production rate, the pressure of the reactor, the pressure and temperature of the separator, and the temperature of stripper unit operations are selected.

5.1. Multiple Models. The selection of MPC parameters need not be optimal, but they should follow the general MPC design rules.[21] In this simulation, the prediction horizon, P, is chosen to be 10 and the control horizon, M, to be 4. Equal weight among the inputs (weight = 1) is used, implying no excessive penalties on the inputs. However, the weights on the outputs are different. The production rate is given the largest weight among the controlled variables. Table 3 lists the weights.

The lower and upper bounds on the inputs are their physical valve position bounds (0−100%). The reactor temperature set point (controlled variable) is confined

to the range 110 °C < T_r < 130 °C with no more than 2 °C change in the set point at each sample time. The maximum allowable rate of change in any valve position is set at 50% at each sample time. The controller sampling period is 6 min to synchronize with the reactor feed and gas analyzers.

The multiple models will be implemented in an MPC design that uses model switching based on the following performance index function[2]

$$J_j(t) \equiv \mu\|\tilde{Y}_j\|^2 + \nu\int_0^t \|\tilde{Y}_j\|^2(\tau)\,\mathrm{d}\tau, \quad \mu, \nu > 0, j = 1, ..., n \tag{38}$$

The term $\tilde{Y}_j$ represents plant/model mismatch for model j. Note that the vector $\hat{Y}_j$ is a subset of the set of controlled variables. In this work, there are only 7 controlled variables in the MPC formulation (not all 41 as listed in Table 13). The above equation incorporates both instantaneous and long-term measures of accuracy. The design parameters μ and ν are selected to have a value between 1 and 0, respectively, to balance the tradeoff between these two extremes. The fixed-parameter model used by the MPC will be the one with the smallest performance index.

5.1.1. Regulation. Most of the disturbances listed in Table 9 can be compensated for by first closing the three level loops and using the reactor cooling water to control the reactor temperature. It is well recognized that the disturbance named IDV(6), which represents a loss in the A feed, is very difficult to address in almost all of the proposed control strategies in the open literature. An MPC was developed based on a single fixed-parameter model identified at mode 3. The closed-loop performance (not shown) in the presence of IDV(6) was unable to regulate the system. It will be shown subsequently that IDV(6) can be compensated for satisfactorily by using multiple fixed-parameter models in an MPC framework.

The multiple fixed-parameter linear models are obtained by linearization of the nonlinear TE model as described in section 4 at selected operating modes. The number of states of each linear model at each mode is 40. The MPC design will be based on these linear fixed models. Figure 2 shows the response of some of the more important variables in the presence of IDV(6) when the system is at operating mode 3 (90/10). It is found that the controlled variables approach a stable steady state that is not the original steady-state associated with operating mode 3. To maintain the desired production rate, the flow rate of A + C feed (stream 4, not shown) is increased, which, in turn, will result in an increase in all (the reactor, separator, and stripper) the pressures and in the purge rate. The bottom left panel in Figure 2 shows that the purge valve is wide open in an attempt to stabilize the pressures.

The production rate (middle left panel) shows a decrease in the production for about 18 h. The rate of decrease is ~4.25%, which is an improvement when compared to the solution given in ref 10 (in their work, the production rate set point is decreased by 23.8%). It is observed from the graph of the operating cost (middle right panel) that the cost has increased 7-fold. The graph in the bottom right panel shows that the linear model identified at mode 2 (10/90) is selected to be the final model of choice (the model that gave the smallest performance index).

It is not surprising that the MPC strategy based on fixed-parameter models, one each for 50/50 (base case), 10/90 (mode 2), and 90/10 (mode 3) operating conditions, cannot compensate effectively for the IDV(6) disturbance. The process is highly nonlinear, with multiple interactions and constraints on the manipulated variables.

5.1.2. Transition Control. The TE process is required to operate at more than one operating mode and at three different G/H mass ratio product grades (see Table 1). Transition control is examined at three modes: the base case (mode 0) and modes 2 and 3. The transition control results shown in Figure 3 are not based on minimizing the operational costs but rather on permitting stable and fast transitions.

Transition from Mode 0 to Mode 2. The reference trajectories of the controlled variables are selected to be first-order responses. From Figure 3, it is observed that the pressure responses of the reactor and separator are satisfactory. The mole percent of G in the product stream (middle right panel) shows that the controller can achieve the desired product ratio in a reasonable amount of time (~8 h). The production rate and the operating cost are shown in the bottom panels. It is observed that the operating cost reaches a steady value of $340/h in ~13 h and that the production rate at the start and at the end are nearly the same value. Not shown is the E feed valve, which is ~99% percent open to achieve the transition.

Transition from Mode 0 to Mode 2 to Mode 3. Most of the control solutions that appear in the open literature indicate that repeated transitions are very difficult to accomplish. Here, the objective is to realize multiple transitions: from mode 0 (base case) to mode 2 to mode 3 (G/H ratio from 50/50 → 10/90 → 90/10).

Figure 4 shows the closed-loop performance of the system during multiple transitions. As in the previous single transition, satisfactory pressure control is not difficult to achieve. The mole percent of G in the product stream (middle right panel) shows a larger tracking error when the system transitions from mode 2 to mode 3 compared to when it transitions from mode 0 to mode 2. One possible reason is the sharp change in the reference trajectory from mode 2 to mode 3. A less sharp reference trajectory will reduce the tracking error. During the transition, the calculated E feed valve (not shown) is clamped at its upper limit for about 18 h.

It is interesting to analyze the accompanying operating cost curve. The operating cost (bottom right panel) at mode 0 is about $165/h; at mode 2, the cost reaches its highest peak of $340/h and then decreases to a value of $220/h at about 36 h after the start of the transition. The subsequent increase after 36 h is due to an increase in the purge rate (not shown). After 40 h, the operating cost converges to a steady state of about $230/h.

5.2. State-Shared Model. A state-shared modeling approach for transition control of continuous systems was developed in refs 2 and 23−25. The state-shared model is a nonminimal realization such that while all of the models share the same state-space representation, the parameters of each model's measurement equation are adapted.

Theorem 1. Any stable, controllable, and observable m-input/m-output linear time-invariant (LTI) system given by

$$\mathbf{Y}_p(s) = \mathbf{H}(s)\,\mathbf{U}(s) = \mathbf{D}^{-1}(s)\,\mathbf{N}(s)\,\mathbf{U}(s) \tag{39}$$

with $\mathbf{D}(s) = \mathbf{d}(s)\,\mathbf{I}_m$, and $\mathbf{d}(s)$, a polynomial of degree n,

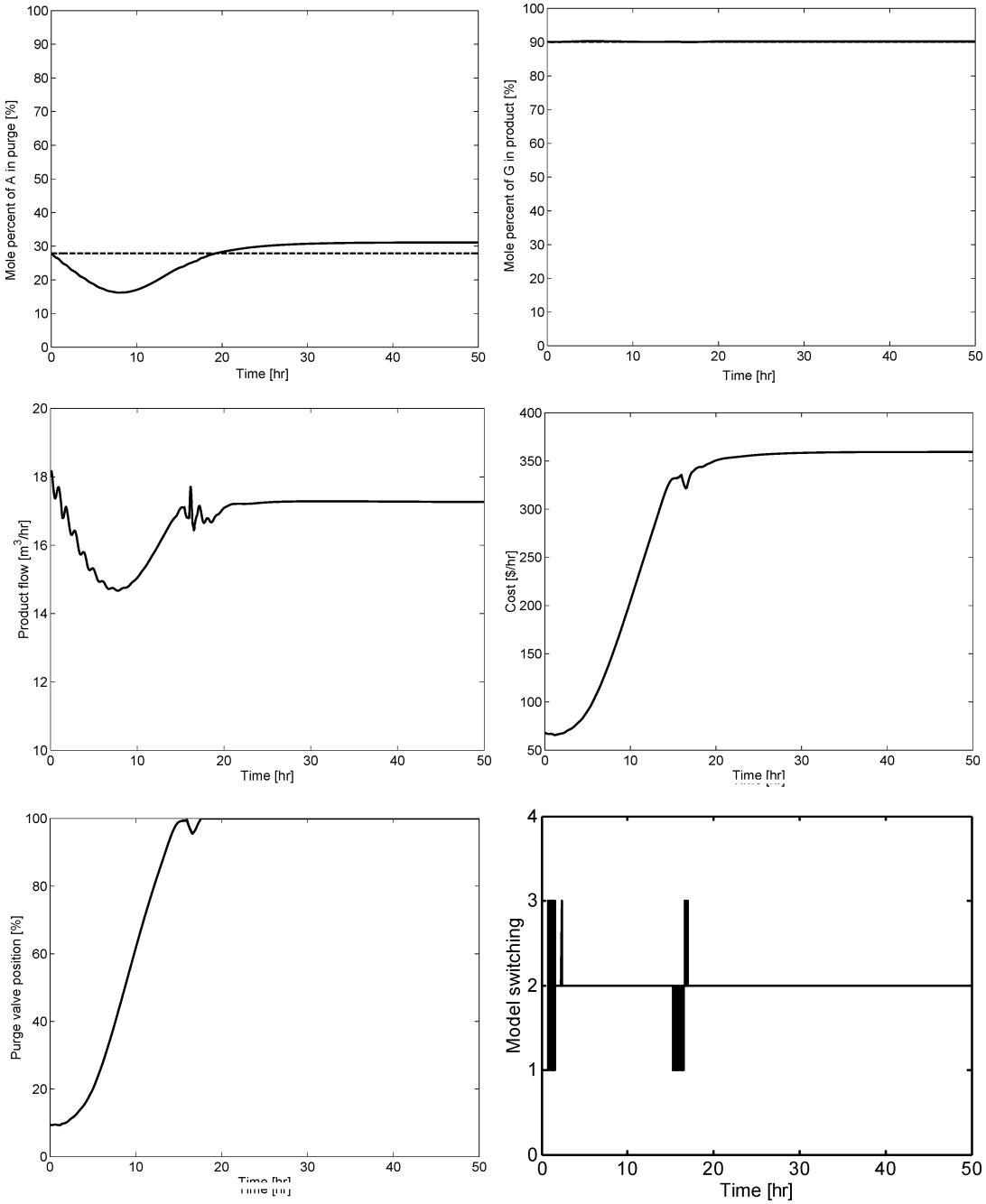

Figure 2. Multiple fixed models and MPC regulation for A feed loss. The dashed line represents the steady-state value at operating mode 3 (90/10). Top panel: mole percent of A in the purge and mole percent of G in the product. Middle panel: production rate and the operating cost. Bottom panel: purge valve and model switching policy.

is input/output equivalent to the LTI system described by the differential equations

$$\dot{\mathbf{\Omega}}_1 = \mathbf{F}\mathbf{\Omega}_1 + \mathbf{G}\mathbf{U} \qquad \mathbf{\Omega}_1 \in R^{nm\times 1}$$

$$\dot{\mathbf{\Omega}}_2 = \mathbf{F}\mathbf{\Omega}_2 + \mathbf{G}\mathbf{Y}_p \qquad \mathbf{\Omega}_2 \in R^{nm\times 1} \tag{40}$$

and the algebraic equation

$$\mathbf{Y}_p = \mathbf{\Theta}^T\mathbf{\Omega} \tag{41}$$

by suitable choice of the parameter vector $\mathbf{\Theta} \in R^{2nm\times m}$. The pair ($\mathbf{F}$, $\mathbf{G}$) should be controllable with $\mathbf{F} \in R^{nm\times nm}$, an asymptotically stable matrix, and $\mathbf{G} \in R^{nm\times m}$. Given $\mathbf{D}(s)$ and $\mathbf{N}(s)$, the parameter vector $\mathbf{\Theta}$ exists and can be uniquely determined.[25]

Remark 1. The value of $\mathbf{\Theta}$ depends on the pair ($\mathbf{F}$, $\mathbf{G}$) and the coefficients of $\mathbf{H}(s)$. Because $\mathbf{F}$ and $\mathbf{G}$ are under the influence of the designer, $\mathbf{\Theta}$ is uniquely determined based on the known $\mathbf{H}(s)$.

Remark 2. $\mathbf{D}(s)$ is block diagonal, with the same elements in each block. As a result, there are only n elements to be identified to determine $\mathbf{\Theta}_2$; the others are zeros. There are nm^2 elements in $\mathbf{\Theta}_1$; the total number of parameters to be identified is then $n(m^2 + 1)$. For the SISO case where $m = 1$, the number of parameters is $2n$.

The state-shared model is developed using three fixed-parameter models (identified at the base mode and modes 2 and 3) and a reinitialized adaptive model. The latter is a type of adaptive model that begins its adaptation starting with the parameter values of the

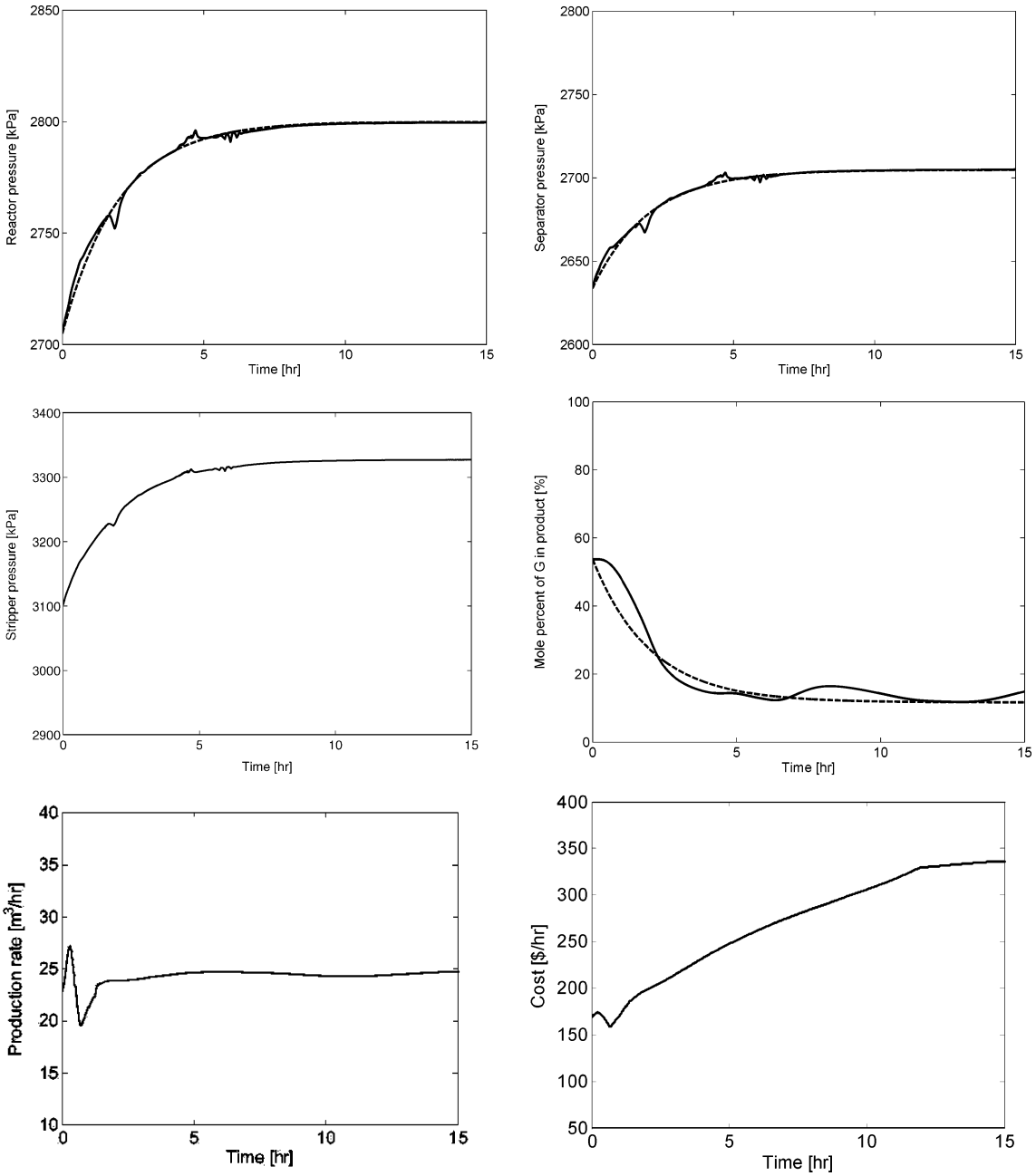

Figure 3. Transition control from mode 0 to mode 2. The dashed line represents the reference trajectory. Top panel: reactor and separator pressures. Middle panel: stripper pressure and mole percent of G in the product. Bottom panel: production rate and operating cost.

fixed-parameter model that gives the smallest estimation error.[26]

At any unknown operating point, an input/output description can be obtained by adapting the coefficients of the measurement equation (eq 41) in the state-shared model. The state-shared model is itself a continuous nonminimal realization of a set of input/output descriptions. These descriptions can be transformed to a matrix fraction description (MFD) using the methods provided in ref 27. Assume that the m-input/m-output system admits an MFD form given by

$$\mathbf{H}(s) = \mathbf{D}^{-1}(s)\,\mathbf{N}(s), \quad \mathbf{D}(s) = \mathbf{d}(s)\,\mathbf{I}_p \tag{42}$$

The order of the denominator of the MFD form of the transfer function, in the case of the TE problem, is 40 ($n = 40$). Using any of the realization approaches,[27] the MFD can be transformed into a controllable canonical,[28] for obvious reasons. The order of this realization is 200 for $m = 5$ input/output pairs (see section 5). The transfer function can also be realized in a state-shared model form given in eq 40. The order of the state-shared model is 400 ($2mn = 2 \times 40 \times 5 = 400$), and the total number of parameters to be adapted is 1040 [$n(m^2 + 1) = 40(5^2 + 1) = 1040$]. This number may appear to be large, but the reader should keep in mind that an entire plant is being discussed. All of the roots of the characteristic polynomial of matrix **F** are placed in the left half complex plane such that the state-shared model is stable. The stability and convergence of the adaptation algorithm are presented elsewhere and will not be repeated.[24,25]

5.2.1. Transition Control. For implementation purposes, it is desirable to keep the order of the model used in the MPC formulation as low as possible. The first step is to reduce the number of input/output pairs.

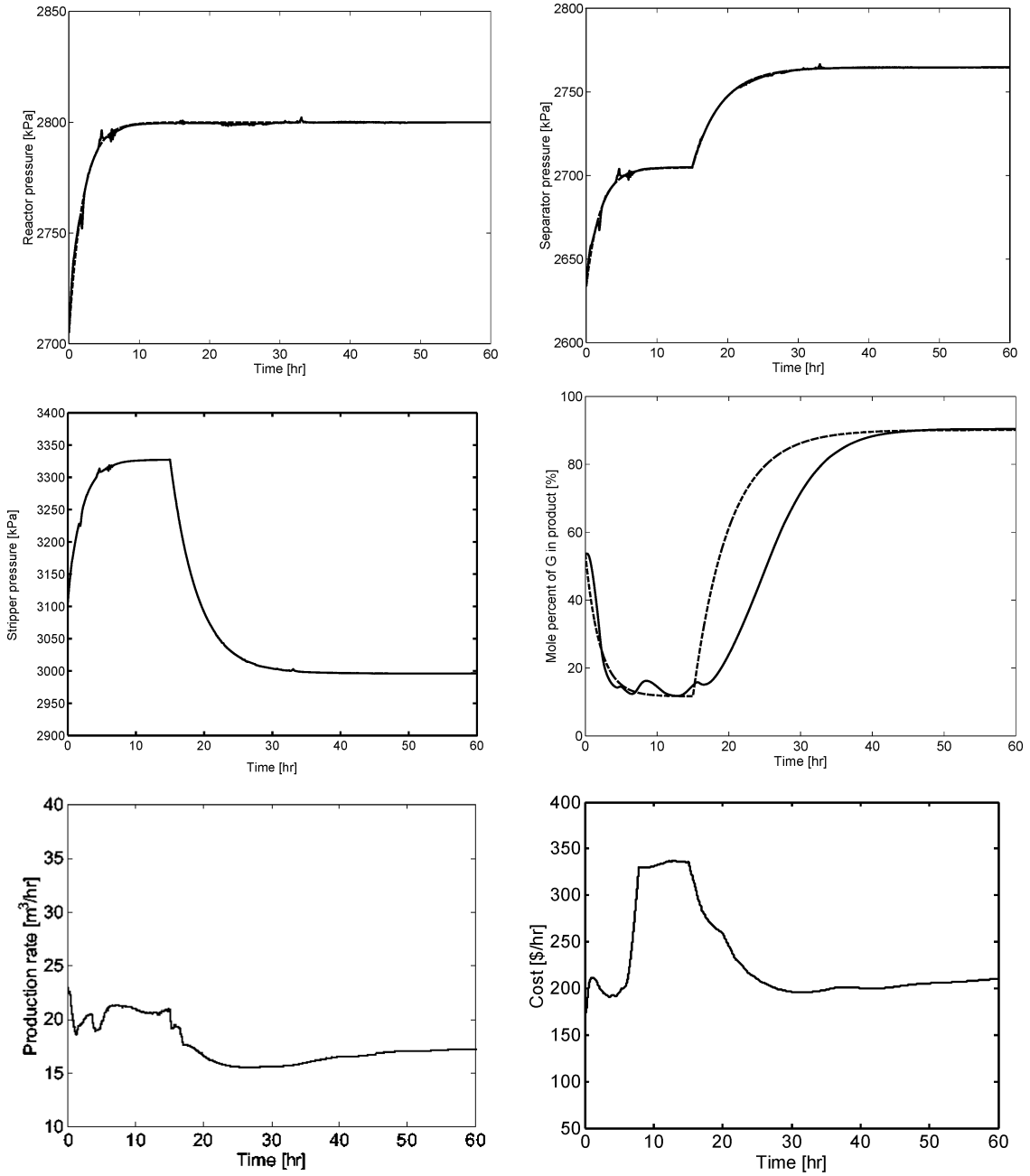

Figure 4. Transition control from mode 0 to mode 2 to mode 3. The dashed line represents the reference trajectory. Top panel: reactor and separator pressures. Middle panel: stripper pressure and mole percent of G in the product. Bottom panel: production rate and operating cost.

Because the agitator speed, XMV(12), only affects the heat-transfer coefficient in the reactor, it is set to a constant value. As before, the manipulated variables XMV(1) (D feed valve), XMV(7) (separator bottoms valve), and XMV(8) (stripper bottoms valve) are expended to control the three levels (the reactor, separator, and stripper) and XMV(10) will control the reactor temperature. From mode 0 to mode 2, the set points of the separator and stripper levels are kept constant (50%); however, the reactor level changes from 75% to 65% during this transition. Thus, a first-order reference trajectory is chosen for the reactor level to make the transition from 75% to 65% of the total reactor volume.

Because mode 2 is obtained at minimum cost, it is reasonable to close the compressor bypass valve XMV(5) and the stripper steam valve XMV(9). In this work, two first-order reference trajectories are chosen to permit XMV(5) and XMV(9) to close smoothly when the system transitions from mode 0 to mode 2. This removes 2 more control degrees of freedom, leaving 6 unassigned.

The ratio of XMV(1) (D feed valve) and XMV(2) (E feed valve) is used to control the G/H product ratio; this removes 1 more control degree of freedom. The remain 5 control degrees of freedom are XMV(3), XMV(4), XMV(6), the set point of the reactor temperature, and XMV(11). Five controlled variables are selected for regulation; they are the production rate, the reactor pressure, the separator temperature and pressure, and the stripper temperature.

The MPC prediction and controller horizons, as well as the choice of the weights among the inputs, the bounds on the inputs, and the bound on their rate of change, are unchanged. However, the weights among the outputs are adjusted to obtain satisfactory performance. In this case, the output weights are given by Table 4.

Table 4. Output Weighting

variable	output weight
reactor pressure	0.15
separator temperature	1.0
separator pressure	0.1
production rate	2.0
stripper temperature	0.2

Figure 5 shows the closed-loop performance as the system transitions from mode 0 to mode 2 with the state-shared model in a MPC formulation (SSMPC). It is observed that the responses of the reactor and separator pressures are satisfactory. Also, the stripper pressure does not become unstable even though it is not a controlled variable. The graph of the mole percent of G in the product (middle right panel) shows that the product ratio change is smooth and, at 7.5 h after the initial request for a transition, it reaches the set point of mode 2. Not shown is the E feed valve, which changes smoothly and never reaches its upper bound. The production rate and the operating cost are shown in the bottom panels. The operating cost reaches a value of \$183.8/h after 12 h. The production rate goes to the set point of 22.73 m^3/h at mode 2.

As a convenience to the reader, the set points of the controlled variables in mode 2 are restated. They are as follows: reactor pressure, 2800 kPa; reactor temperature, 124.21 °C; reactor level, 65%; separator temperature, 90.26 °C; separator level, 50%; separator pressure, 2705 kPa; stripper level, 50%; production rate, 22.73 m^3/h; stripper temperature, 65.39 °C; purge mole % A, 36.63%; product mole % G, 11.66%.

To further compare the fixed model MPC strategy and state-shared MPC strategy, the input/output pairs and the same set-point trajectories that were used with the

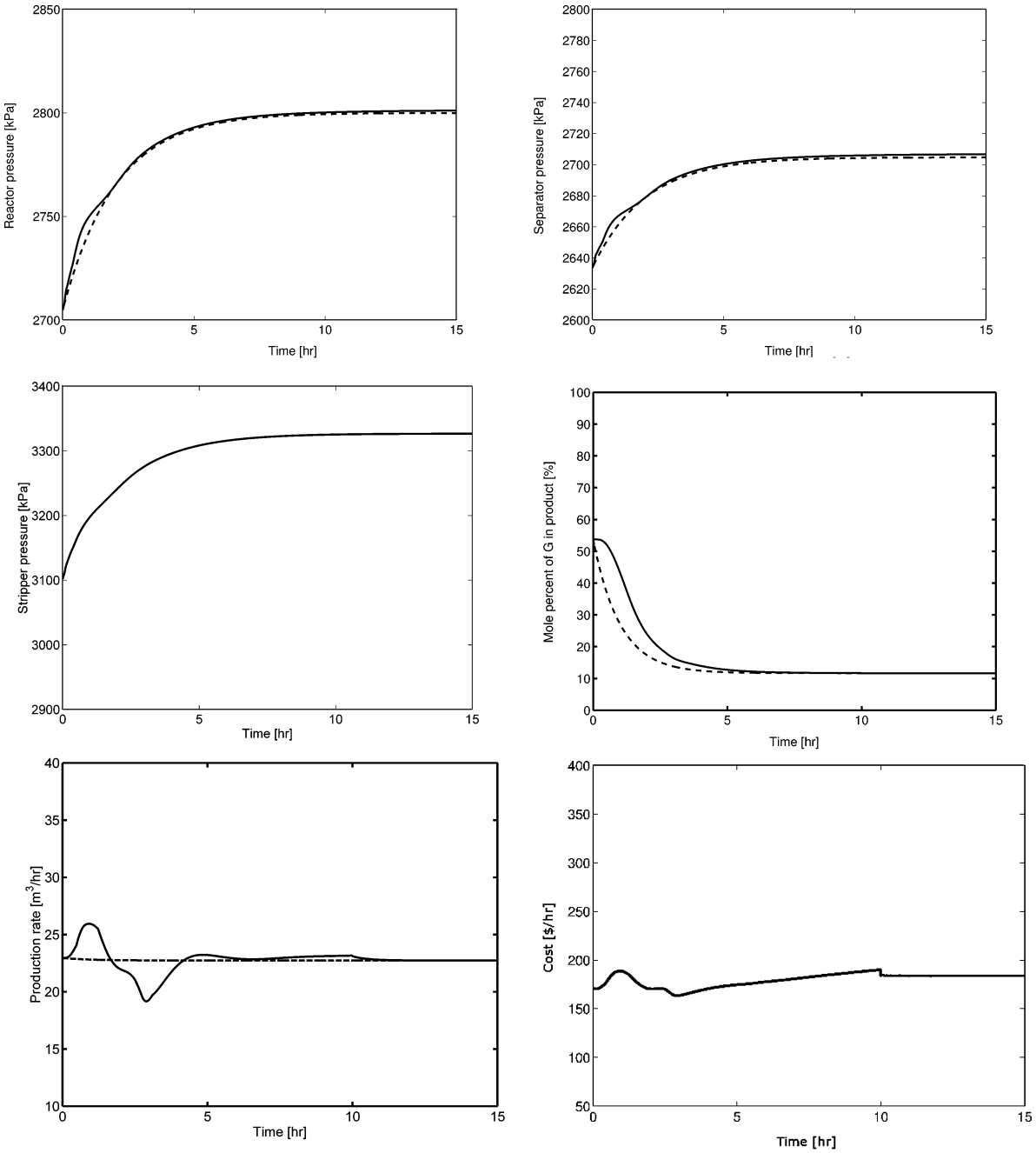

Figure 5. Transition control from mode 0 to mode 2 with SSMPC. The dashed line represents the reference trajectory. Top panel: reactor and separator pressures. Middle panel: stripper pressure and mole percent of G in the product. Bottom panel: production rate and operating cost.

Table 5. Notation and Definition I

variable	units	definition
AD(i), BD(i), CD(i)	i = A, ..., H	coefficients in the density formulation
AH(i), BH(i), CH(i)	i = A, ..., H	coefficients in the liquid enthalpy formulation
AG(i), BG(i), CG(i), AV(i)	i = A, ..., H	coefficients in the vapor enthalpy formulation
C_{pc}	Btu/lb·mol·K	cooling water heat capacity
$\hat{C}_{pr}$	Btu/lb·mol·K	specific molar heat capacity of a liquid mixture in the reactor
$\hat{C}_{ps}$	Btu/lb·mol·K	specific molar heat capacity of a liquid mixture in the separator
$\hat{C}_{pc}$	Btu/lb·mol·K	specific molar heat capacity of a liquid mixture in the stripper
$\hat{C}_{pv}$	Btu/lb·mol·K	specific molar heat capacity of a gas mixture
E_i, i = 1, ..., 4	cal/mol	activation energy of reaction i
F_i	lb·mol/h	flow rate of stream i
F_{wr}	lb·mol/h	flow rate of the cooling water
H_r	Btu	enthalpy in the reactor
MW_i	g/lb·mol	molecular weight of component i
MWS_i	g/lb·mol	molecular weight of stream i
$N_{i,c}$	lb·mol	mole numbers of component i in the stripper
$N_{i,r}$	lb·mol	mole numbers of component i in the reactor
$N_{i,s}$	lb·mol	mole numbers of component i in the separator
$N_{i,v}$	lb·mol	mole numbers of component i in the mixing zone
P	mmHg	pressure
P_o	mmHg	atmospheric pressure
P_r	mmHg	pressure in the reactor
P_s	mmHg	pressure in the separator
P_v	mmHg	pressure in the mixing zone
$P_{i,r}$	mmHg	partial pressure of component i in the reactor
$P_{vp,i}$	mmHg	vapor pressure
Q_{r1}, Q_{r2}	Btu/lb·mol	molar heat of reaction for reactions 1 and 2
Q_{uc}	Btu/h	energy added to the stripper by steam
Q_{ur}	Btu/h	energy removed from the reactor by cooling water
Q_{us}	Btu/h	energy removed from stream 7 by cooling water
T_c	°C	temperature in the stripper
T_{cwr}	°C	outlet cooling water temperature in the reactor
T_{cws}	°C	outlet cooling water temperature in the separator

state-shared MPC formulation are applied to the fixed model strategy. The results for the transition between modes 0 and 2 (not shown) indicate that the reactor and separator pressures and the product quality (mole % G) are regulated to their set points (the stripper pressure is regulated but is not a controlled variable) and the production cost is $180/h. However, the production rate did not track its reference trajectory well (below the reference trajectory). The results for the transition among modes 0, 2, and 3 (not shown) show much better regulation of the pressures and the product purity. However, the production rate is below its reference trajectory during the transition from mode 0 to mode 2 (the production cost decreases) and above this trajectory during the transition from mode 2 to mode 3 (the production cost increases). A primary reason for this behavior is the inaccuracy of the fixed models. Clearly, when the models are adapted as in the state-shared MPC strategy, this behavior is mitigated.

6. Summary

In this work, two approaches to plantwide control synthesis were demonstrated on the TE challenge process. Because both control methods rely on a model of the plant and because the computer programs provided by Downs and Vogel[1] cannot be used directly for an MPC design, a mechanistic model based on first principles was developed using all of the information provided in ref 1 and Downs and Vogel's Fortran programs. The results of the system of nonlinear differential−algebraic equations are validated with data obtained from the original Fortran programs.

The first model-based control formulation employed multiple fixed-parameter models and switching, while the second control formulation used an adaptive state-shared model. Both plantwide model-based control

Table 6. Notation and Definition II

variable	units	definition
T_{in}	°C	inlet temperature of the reactor cooling water
T_k	K	273.15
T_{out}	°C	outlet temperature of the reactor cooling water
T_r	°C	temperature in the reactor
T_s	°C	temperature in the separator
$T_{st,i}$	°C	temperature of the stream i, i = 1, ..., 11
T_v	°C	temperature in the mixing zone
UA	Btu/K·h	product of the heat-transfer coefficient and area
$V_{L,r}$	ft^3	liquid volume in the reactor
$V_{v,r}$	ft^3	vapor volume in the reactor
V_{cool}	ft^3	cooler volume
W_c	Btu/h	power of compressor
XMV(i)	%	valve position, i = 1, ..., 11
XMV(12)	%	agitator speed
f_{T_c}		temperature factor of the split fraction
h_j	Btu/lb·mol	specific molar enthalpy in stream j
h_c	Btu/lb·mol	specific molar enthalpy in the stripper
h_r	Btu/lb·mol	specific molar enthalpy in the reactor
h_s	Btu/lb·mol	specific molar enthalpy in the separator
h_v	Btu/lb·mol	specific molar enthalpy in the mixing zone
$\dot{m}_c$	kg/h	cooling water mass flow rate
v_{ag}		dimensionless agitator speed
$x(i)$		mole fraction of component i in the liquid
x_r		mole fraction in the reactor
x_p		states of the state-space model
$y(i)$		mole fraction of component i in the vapor
y_p		vector of outputs of the TE plant
Φ_i		split fraction for component i, i = A, ..., H
α_1, α_2		coefficients in the reaction rate
β_1, β_2, β_3		coefficients in the reaction rate
ρ_c	lb·mol/ft^3	cooling water molar density in the reactor cooling system
ρ_s	lb·mol/ft^3	cooling water molar density in the condenser
ρ_{liq}	lb·mol/ft^3	liquid mixture density
χ_i		valve position, i = 1, 2, ..., 11
χ_{agCap}		fraction of the maximum agitator capacity

Table 7. Process Manipulated Variables

variable name	variable no.	base case value (%)	low limit	high limit	units
D feed flow (stream 2)	XMV(1)	63.053	0	5811	kg/h
E feed flow (stream 3)	XMV(2)	53.980	0	8354	kg/h
A feed flow (stream 1)	XMV(3)	24.644	0	1.017	kscmh
A and C feed flow (stream 4)	XMV(4)	61.302	0	15.25	kscmh
component recycle valve	XMV(5)	22.210	0	100	%
purge valve (stream 9)	XMV(6)	40.046	0	100	%
separator liquid flow (stream 10)	XMV(7)	38.100	0	65.71	m^3/h
stripper liquid flow (stream 11)	XMV(8)	46.534	0	49.10	m^3/h
stripper steam valve	XMV(9)	47.446	0	100	%
reactor cooling water flow	XMV(10)	41.106	0	227.1	m^3/h
condenser cooling water flow	XMV(11)	18.114	0	272.6	m^3/h
agitator speed	XMV(12)	50.000	150	250	rpm

Table 8. Process Operating Constraints

			normal operating limits	shutdown limits
process variable	low	high	low	high
reactor pressure	none	2985 kPa	none	3000 kPa
reactor level	50%	100%	2.0 m^3	24.0 m^3
	11.8 m^3	21.3 m^3		
reactor temperature	none	150 °C	none	175 °C
separator level	30%	100%	1.0 m^3	12.0 m^3
	3.3 m^3	9.0 m^3		
stripper base level	30%	100%	1.0 m^3	8.0 m^3
	3.5 m^3	6.6 m^3		

Table 9. Process Disturbances

ref no.	description	signal type
IDV(1)	A/C feed ratio, B composition constant (stream 4)	step
IDV(2)	B composition, A/C ratio constant (stream 4)	step
IDV(3)	D feed temperature (stream 2)	step
IDV(4)	reactor cooling water inlet temperature	step
IDV(5)	condenser cooling water inlet temperature	step
IDV(6)	A feed loss (stream 1)	step
IDV(7)	C header pressure loss-reduced availability (stream 4)	step
IDV(8)	A, B, and C feed composition (stream 4)	random
IDV(9)	D feed temperature (stream 2)	random
IDV(10)	C feed temperature (stream 4)	random
IDV(11)	reactor cooling water inlet temperature	random
IDV(12)	condenser cooling water inlet temperature	random
IDV(13)	reaction kinetics	slow drift
IDV(14)	reactor cooling water	valve sticking
IDV(15)	condenser cooling water	valve sticking

Table 10. Coefficients in the Antoine Equation for Condensable Components

component	A	B	C
D	15.92	−1440	259.0
E	16.35	−2114	265.5
F	16.35	−2114	265.5
G	16.43	−2748	232.9
H	17.21	−3318	249.6

strategies are linear. The multiple fixed-parameter model approach was demonstrated for regulation and single and multiple transitions. The regulation selected is considered the worst disturbance: the loss of the A feed. It was shown that this strategy was able to provide a satisfactory closed-loop performance. Transition control was demonstrated for two cases: mode 0 to mode 2 and mode 0 to mode 2 to mode 3.

The second adaptive state-shared model approach was demonstrated for single mode transition from mode 0 to mode 2. A better transition control result was found when compared with the first approach based on the quality of the control action and operating costs.

Table 11. Nominal Values of Stripper Splits for the Exiting Vapor Stream

Φ_A	Φ_B	Φ_C	Φ_D	Φ_E	Φ_F	Φ_G	Φ_H
0.995	0.991	0.990	0.916	0.936	0.938	0.058	0.030

Table 12. Parameters in the Reaction Rate Equations

parameter	value
α_1	1.1544
α_2	0.3735
β_1	31.585 953 6
β_2	3.000 940 14
β_3	53.406 044 3
β_4	53.141 412 3
E_1	40 000.0 cal/mol
E_2	20 000.0 cal/mol
E_3	60 000.0 cal/mol
E_4	60 000.0 cal/mol
R	1.987 cal/mol·K
Q_{r1}	−0.068 993 810 54 Btu/lb·mol
Q_{r2}	−0.05 Btu/lb·mol
Q_{r3}	not given, assumed to be 0
Q_{r4}	not given, assumed to be 0

Acknowledgment

Z.T. was supported by NSF grant CTS-9703252.

Appendix

TE Process Description. The information that appears in this appendix also appears in refs 1 and 6. It is repeated here, mostly in tabular form, for the convenience of the reader. Tables 5 and 6 provide the definitions of the notation.

The TE process has 12 manipulated variables; these are listed in Table 7. The high and low shutdown limits are part of the plant's safety interlock system. The given process constraints are provided in Table 8.

There are 15 possible disturbances; these are listed in Table 9.

According to ref 1, the total operating costs in this paper are given by

$$\begin{aligned}\text{costs} = {} & 0.0536\,\frac{\$}{\text{kWh}}\,Y(20) + 0.0318\,\frac{\$}{\text{kg}}\,Y(19) + \\ & 44.791\,\frac{\text{kgmol h}^{-1}}{\text{kscmh}}\,Y(10)\left[22.06\,\frac{\$}{\text{kmol}}\,Y(29) + \right. \\ & 6.177\,\frac{\$}{\text{kmol}}\,Y(31) + 22.06\,\frac{\$}{\text{kmol}}\,Y(32) + \\ & 14.56\,\frac{\$}{\text{kmol}}\,Y(33) + 17.89\,\frac{\$}{\text{kmol}}\,Y(34) + \\ & \left. 30.44\,\frac{\$}{\text{kmol}}\,Y(35) + 22.94\,\frac{\$}{\text{kmol}}\,Y(36)\right]/100 + \\ & 9.21\,\frac{\text{kgmol}}{\text{m}^3}\,Y(17)\left[22.06\,\frac{\$}{\text{kmol}}\,Y(37) + \right. \\ & \left. 14.56\,\frac{\$}{\text{kmol}}\,Y(38) + 17.89\,\frac{\$}{\text{kmol}}\,Y(39)\right]/100 \quad \text{(A.1)}\end{aligned}$$

Table 13. Measured Output Variables (from Reference 6)

	measured value	mode 0 (base case)	mode 1 (50/50)	mode 2 (10/90)	mode 3 (90/10)	mode 4 (50/50)	mode 5 (10/90)	mode 6 (90/10)
1	A feed, kscmh	0.251	0.267	0.309	0.194	0.503	0.325	0.219
2	D feed, kg/h	3664	3657	734	5179	5811	761	5811
3	E feed, kg/h	4509	4440	8038	700	7244	8354	788
4	A + C feed, kscmh	9.35	9.24	8.55	7.83	14.73	8.83	8.79
5	recycle flow, kscmh	26.90	32.18	31.69	19.67	29.22	31.27	20.08
6	reactor feed, kscmh	42.34	47.36	46.08	32.09	53.76	46.24	34.02
7	reactor pressure, kPa	2705	2800	2800	2800	2800	2800	2800
8	reactor level, %	75	65	65	65	65	65	65
9	reactor temp, °C	120.4	122.9	124.2	121.9	128.2	124.6	123
10	purge rate, kscmh	0.337	0.211	0.361	0.087	0.462	0.384	0.099
11	separator temp, °C	80.1	91.7	90.3	83.4	74.1	88.9	80.9
12	separator level, %	50	50	50	50	50	50	50
13	separator pressure, kPa	2634	2706	2705	2765	2699	2705	2761
14	separator underflow, m^3/h	25.16	25.28	26.31	17.55	40.06	27.45	19.60
15	stripper level, %	50	50	50	50	50	50	50
16	stripper pressure, kPa	3102	3326	3327	2996	3365	3330	3015
17	stripper underflow, m^3/h	22.95	22.89	22.73	18.04	36.04	23.55	20.20
18	stripper temp, °C	65.73	66.5	65.4	62.3	51.5	63.9	60.5
19	steam flow, kg/h	230	4.74	4.90	5.34	6.87	5.11	5.59
20	component work, kW	341	278.9	274.7	272.6	263.2	271.l7	293.2
21	reactor cooling temp, °C	94.6	102.4	108.6	101.9	96.6	108.5	100.6
22	condensor cooling temp, °C	77.3	92.0	91.6	45.0	73.5	89.8	45.7
23	feed % A, mol %	32.19	32.21	34.82	29.46	35.40	34.78	29.99
24	feed % B, mol %	8.89	14.93	8.18	27.74	8.78	7.85	26.34
25	feed % C, mol%	26.38	18.75	19.43	17.97	22.36	19.54	18.80
26	feed % D, mol %	6.88	6.03	1.20	12.68	7.95	1.24	13.23
27	feed % E, mol %	18.78	16.71	25.47	3.86	17.01	26.03	3.91
28	feed % F, mol %	1.66	4.04	5.60	1.29	3.88	5.60	1.33
29	purge % A, mol %	32.96	32.73	36.63	27.86	40.94	36.71	28.61
30	purge % B, mol %	13.82	21.83	11.77	45.07	15.90	11.47	44.41
31	purge % C, mol %	23.98	13.11	14.63	9.22	15.68	14.57	9.76
32	purge % D, mol %	1.26	0.90	0.13	2.18	0.68	0.13	2.09
33	purge % E, mol %	18.58	16.19	22.37	3.94	15.41	22.92	4.00
34	purge % F, mol %	2.26	5.39	7.37	1.82	5.72	7.44	1.91
35	purge % G, mol %	4.84	6.62	1.32	9.40	3.85	1.26	8.76
36	purge % H, mol %	2.30	3.23	5.79	0.50	1.82	5.51	0.46
37	product % D, mol %	0.02	0.01	0.00	0.03	0.02	0.00	0.03
38	product % E, mol %	0.84	0.58	0.92	0.16	1.21	1.01	0.18
39	product % F, mol %	0.01	0.19	0.29	0.07	0.04	0.32	0.08
40	product % G, mol %	53.72	53.83	11.66	90.09	53.35	11.65	90.07
41	product % H, mol %	43.83	43.91	85.64	8.17	43.52	85.53	8.16

where Y represents 41 measurements (see Table 13). The first item is the compressor operating cost, the second item is the steam cost, the third item is the purge losses, and the final item is the losses in the production. All coefficients given in eq A.1 were provided in ref 1.

The coefficients for the Antoine equation, eq 3, and the nominal values for the stripper splits, eq 32, are given in Tables 10 and 11, respectively. The reaction parameters for eq 7 are given in Table 12.

For this multiple input/multiple output system, the values of the manipulated variables and measurements that give the required G/H mass ratios are not unique. Ricker[6] provided the optimal steady-state operating conditions for all of the operating modes. These values are listed in Table 13. The optimal steady-state values are also provided.

Literature Cited

(1) Downs, J. J.; Vogel, E. F. A plant-wide industrial process control problem. *Comput. Chem. Eng.* **1993**, *17* (3), 245−255.

(2) Tian, Z.; Hoo, K. A. Transition control using a state-shared model approach. *Comput. Chem. Eng.* **2003**, *27* (11), 1641−1656.

(3) Ye, N.; McAvoy, T. J.; Kosanovich, K. A.; Piovoso, M. J. Plant wide control using an inferential approach. *Proceedings of the American Control Conference*, San Francisco, CA, June 1993; Vol. 2, pp 1900−1904.

(4) Ye, N.; McAvoy, T. J.; Kosanovich, K. A.; Piovoso, M. J. Optimal averaging level control for the tennessee eastman problem. *Can. J. Chem. Eng.* **1995**, 234−240.

(5) Luyben, W. L.; Tyreus, B. D.; Luyben, M. L. *Plantwide Process Control*; McGraw-Hill: New York, 1998.

(6) Ricker, N. L. Optimal steady-state operation of the Tennessee Eastman challenge process. *Comput. Chem. Eng.* **1995**, *19* (9), 949−959.

(7) Ricker, N. L.; Lee, J. H. Nonlinear model predictive control of the Tennessee Eastman challenge process. *Comput. Chem. Eng.* **1995**, *19* (9), 961−981.

(8) Ricker, N. L.; Lee, J. H. Nonlinear modeling and state estimation for the Tennessee Eastman challenge process. *Comput. Chem. Eng.* **1995**, *19* (9), 983−1005.

(9) Ricker, N. L. Decentralized control for the Tennessee Eastman challenge process. *J. Process Control* **1996**, *6*, 205−221.

(10) McAvoy, T. J.; Ye, N. Base control for the Tennessee Eastman problem. *Comput. Chem. Eng*. **1994**, *18* (5), 383−413.

(11) Ogunnaike, B. A.; Ray, W. H. *Process Dynamics, Modeling, and Control*; Oxford Press: Oxford, U.K., 1994.

(12) Banerjee, A.; Arkun, Y. Control configuration design applied to the Tennessee Eastman plantwide control problem. *Comput. Chem. Eng.* **1995**, *19*, 453−480.

(13) Skogestad, S. Plantwide control: the search for the self-optimizing control structure. *J. Process Control* **2000**, *10*, 487−507.

(14) Larsson, T.; Hestetun, K.; Hovland, E.; Skogestad, S. Self-optimizing control of a large-scale plant: The Tennessee Eastman process. *Ind. Eng. Chem. Res.* **2001**, *40* (22), 4889−901.

(15) Larsson, T.; Skogestad, S. Plantwide control: A review and a new design procedure. *Int. J. Control* **2000**, *21* (4), 209−240.

(16) Arbel, A.; Rinard, I. H.; Shinnar, R. Dynamics and control of fluidized catalytic crackers. 3: Designing the control system choice of manipulated and measured variables for partial control. *Ind. Eng. Chem. Res.* **1996**, *35* (7), 2215.

(17) Arbel, A.; Rinard, I. H.; Shinnar, R. Dynamics and control of fluidized catalytic crackers. 4: The impact of design on partial control. *Ind. Eng. Chem. Res.* **1997**, *36* (7), 747.

(18) Shinnar, R.; Dainson, B.; Rinard, I. H. Partial control. a systematic approach to the concurrent design and scale-up of complex processes: The role of control system design in compensating for significant model uncertainties. *Ind. Eng. Chem. Res.* **2000**, *39*, 103−121.

(19) Reklaitis, G. V. *Introduction to Material and Energy Balances*; John Wiley & Sons: New York, 1983.

(20) Kreyszig, E. *Introductory Functional Analysis with Applications*; Wiley Classics Library; John Wiley & Sons: New York, 1989.

(21) Prett, D. M.; Garcia, C. E. *Fundamental Process Control*; Butterworth Publishers: London, 1988.

(22) Seborg, D.; Edgar, T. F.; Mellichamp, D. A. *Process Dynamics and Control*; John Wiley & Sons: New York, 1989.

(23) Tian, Z.; Hoo, K. A. A state-shared modeling approach to transition control. *Proceedings of the IFAC 2003 on Advanced Control of Chemical Processes*; IFAC: Hong Kong, People's Republic of China, 2004.

(24) Tian, Z.; Hoo, K. A. A state-shared model approach for multiple-input multiple-output systems. *IEEE Control Syst. Technol*. **2002**, under review.

(25) Tian, Z.; Hoo, K. A. State-shared model-based control approach to transition control. *Proceedings of the 2003 American Control Conference*, Denver, CO, 2003; pp 5405−5410.

(26) Narendra, K. S.; Balakrishnan, J. Improving transient response of adaptive control systems using multiple models and switching. *IEEE Trans. Autom. Control* **1994**, *39* (9), 1861−1866.

(27) Kailath, T. *Linear Systems*; Prentice-Hall: Englewood Cliffs, NJ, 1980.

(28) Antsaklis, P. J.; Michel, A. N. *Linear System*; McGraw-Hill: New York, 1997.

Received for review April 14, 2004
Revised manuscript received February 4, 2005
Accepted February 7, 2005

IE0496939